Simulation and Mathematical Modelling of Aircraft Flying Qualities with Varying Tail Dihedral

By

Muhammad Uzair Khan

00000171149

Supervisor

Dr. Naveed Akmal Din

DEPARTMENT OF MECHANICAL ENGINEERING

COLLEGE OF ELECTRICAL & MECHANICAL ENGINEERING

NATIONAL UNIVERSITY OF SCIENCES AND TECHNOLOGY

ISLAMABAD

AUGUST, 2019

Simulation and Mathematical Modelling of Aircraft Flying Qualities with Varying Tail Dihedral

Author

Muhammad Uzair Khan

Regn Number

00000171149

A thesis submitted in partial fulfillment of the requirements for the degree of

MS Mechanical Engineering

Thesis Supervisor:

Dr. Naveed Akmal Din

Thesis Supervisor's Signature:_____

DEPARTMENT OF MECHANICAL ENGINEERING

COLLEGE OF ELECTRICAL & MECHANICAL ENGINEERING

NATIONAL UNIVERSITY OF SCIENCES AND TECHNOLOGY, ISLAMABAD

AUGUST, 2019

Declaration

I certify that this research work titled "*Simulation and Mathematical Modelling of Aircraft Flying Qualities with Varying Tail Dihedral"* is my own work. The work has not been presented elsewhere for assessment. The material that has been used from other sources it has been properly acknowledged / referred.

Signature of Student

M Uzair Khan

2016-NUST-Ms-Mech-00000171149

Language Correctness Certificate

This thesis has been read by an English expert and is free of typing, syntax, semantic, grammatical and spelling mistakes. Thesis is also according to the format given by the university.

Signature of Student

Muhammad Uzair Khan

00000171149

Signature of Supervisor

Plagiarism Certificate (Turnitin Report)

This thesis has been checked for Plagiarism. Turnitin report endorsed by Supervisor is attached.

Signature of Student

M Uzair Khan

00000171149

Signature of Supervisor

Copyright Statement

Acknowledgements

I am thankful to my Creator Allah Subhana-Watala to have guided me throughout this work at every step and for every new thought which You setup in my mind to improve it. Indeed I could have done nothing without Your priceless help and guidance. Whosoever helped me throughout the course of my thesis, whether my parents or any other individual was Your will, so indeed none be worthy of praise but You.

I am profusely thankful to my beloved parents who raised me when I was not capable of walking and continued to support me throughout in every department of my life.

I would also like to express special thanks to my supervisor Dr. Naveed Akmal Din for his help throughout my thesis and also for Advanced Theory of Vibrations course which he has taught me. I can safely say that I haven't learned any other engineering subject in such depth than the ones which he has taught.

I would also like to pay special thanks to M Diyan Khan for his tremendous support and cooperation. Each time I got stuck in something, he came up with the solution. Without his help I wouldn’t have been able to complete my thesis. I appreciate his patience and guidance throughout the whole thesis.

I would also like to thank Dr. Hassan Aftab and Dr. Sajid-Ullah Butt for being on my thesis guidance and evaluation committee. I am also thankful to them for their support and cooperation.

Finally, I would like to express my gratitude to all the individuals who have rendered valuable assistance to my study.

Dedicated to my exceptional parents whose tremendous support and cooperation led me to this wonderful accomplishment.

Abstract

Aircraft handling qualities depend on the empennage geometry. The size and position of tails along with the arrangement govern the stability and controllability of the aircraft. However, the empennage also effects the aerodynamic efficiency of the aircraft by producing additional drag force. By increasing the tail size, one can achieve better handling qualities, however, this can negatively impact the aerodynamic efficiency by substantially increasing the drag force. A comparison of different tail setups in terms of their contribution to stability and controllability along with their impact on aerodynamic efficiency is done. The analysis was performed using a Vortex Lattice Method. It was observed that the V-Tails provide best stability and controllability characteristics with the lowest wetted area.

V-tail is a tail geometry setup that provides stability and controllability about longitudinal and directional axes simultaneously. In addition, the setup has less wetted area and interference, thus producing less drag as compared to conventional tails. The dihedral angle of a V-tail determines its contribution to both longitudinal and lateral-directional dynamics. However, there is no well-defined empirical method to compute the most suitable dihedral angle for a V-tail in order to meet the required flying qualities. This work presents a method to select the most appropriate dihedral angle of a V-tail to fulfill the requirements of aircraft flying qualities. Numerical calculations were used to generate a complete flight dynamics model with different tail dihedral angles. Subsequently, damping ratios for longitudinal and lateral-directional modes were extracted from these models. Using a curve fitting technique a polynomial was generated for longitudinal and lateral-directional damping ratios against tail dihedral angle. It was observed that by increasing the tail dihedral the longitudinal damping ratio was reduced. In addition, the lateral-directional damping ratio increased with the increase in tail dihedral angle. The lower bound of the tail dihedral angle was obtained using the lateral-directional damping limit in accordance to the flying qualities. Similarly, the upper bound of the tail dihedral angle was obtained using the longitudinal damping limit. The tail dihedral angle in between these bounds was found to be optimal for adequate longitudinal and lateral-directional flying qualities. In addition, it was observed that the mathematical model was not valid for a different flight dynamics model. This is due to the change in aerodynamic behavior of the aircraft.

Key Words: *Empennage, T-Tails, V-Tails, Inverted Y-Tails, Inverted V-Tails, Vortex Lattice, Stability, Controllability, Vortex lattice, Damping ratio, flight dynamics, flying qualities, Athena VLM, mathematical modelling, curve fitting, tail dihedral.*

Table of Contents

List of Figures

List of Tables

Table of Acronyms

Coefficient	Explanation
C_{Y_p}	Change in side force with change in roll rate
C_{HT}	Horizontal tail volume coefficient
C_{VT}	Vertical tail volume coefficient
S_{HT}	Horizontal tail planform area
L_{HT}	Horizontal tail moment arm
S_{VT}	Vertical tail planform area
L_{VT}	Vertical tail moment arm
S_W	Wing planform area
b_w	Wing span
$\bar{c}_w$	Wing mean aerodynamic chord
R^2	Regression coefficient
C_m	Pitching moment coefficient
C_L	Lift force coefficient
$X_{N.P}$	Neutral point location in x-axis
$X_{C.G}$	Center of gravity location in x-axis
$C_{m_{\delta e}}$	Change in pitching moment with change in symmetric elevator deflection
$C_{n_{\delta r}}$	Change in yawing moment with change in asymmetric rudder deflection
C_{m_α}	Change in pitching moment with change in angle of attack
C_{n_β}	Change in yawing moment with change in sideslip angle
C_{l_β}	Change in rolling moment with change in sideslip angle
C_{L_α}	Change in Lift with change in angle of attack
ω	Natural frequency
ξ	Damping ratio
Γ	Dihedral Angle
θ	Pitch Angle
ψ	Heading Angle
ϕ	Bank Angle
u	Axial Velocity
v	Side Velocity
w	Vertical Velocity
g	Acceleration due to gravity

CHAPTER 1. INTRODUCTION

The research work in this dissertation has been presented in two parts. First part is related to familiarizing with different tail setups. This part also compares different tail setups in terms of stability and controllability of the aircraft along with their effect on aerodynamic efficiency. The objective of this part is to come up with a tail setup that has adequate stability and controllability with minimal effect on aerodynamic efficiency. The second part is related to aircraft tail dihedral angle and flying qualities. The objective of this part is to introduce a method for selecting the most suitable tail dihedral angle for an aircraft at a particular flight condition.

1.1 Background

Empennage design of an aircraft, can significantly impact its stability and controllability. It is based on a number of geometrical parameters such as the planform area, longitudinal location, sweep angle and tail dihedral, and consists of multiple surfaces. The arrangement and size of all these surfaces significantly affect the complete dynamics of the aircraft. An aircraft can exhibit better stability and controllability, if the tail planform area is increased. However, the increase in tail planform area increments the drag produced and hence, lowers the aerodynamic efficiency of the aircraft.

1.1.1 Aerodynamics of Tails

Tails are located at the aft most part of fuselage. Tails act as stabilizers which implies that tails are responsible for stabilizing the aircraft by producing restoring forces and moments. The aircraft can move in 6-DOF which includes three positions (x, y, z) and three angular rotations (ϕ, θ, ψ). Any change in these 6-DOF would be due to a change in angle of attack ($\boldsymbol{\alpha}$) or sideslip angle (β) of the wing. Conventionally, if we have a tailless aircraft then it would not be able to come back to its equilibrium position. Therefore, whenever the aircraft is disturbed (wind gust, wind gradients or turbulent air) then tails are responsible for bringing the aircraft back to equilibrium position.

There are three axes (longitudinal, lateral and vertical) of an aircraft as shown in Fig 1.1. Any rotation about longitudinal, lateral and directional axis is known as roll, pitch and yaw respectively. At the aft of fuselage conventionally an aircraft has vertical and horizontal tail which act as stabilizers.

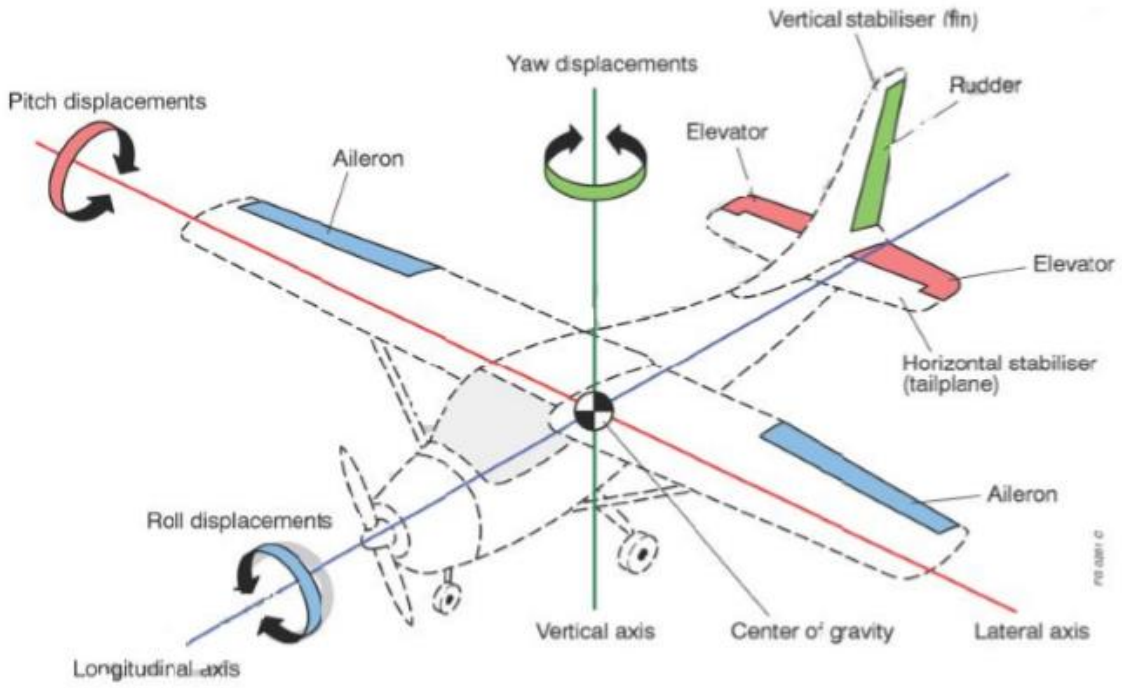

Figure 1.1: Aircraft geometry with conventional tails.

The angle that the lifting surface (horizontal tail, wing etc.) makes with the horizontal plane is known as dihedral angle. As shown in Fig 1.2. Tail location is also an important parameter, it defines the moment arm (distance between C.G. of aircraft and tail aerodynamic center) of the stabilizer and the control surface. The greater the moment arm greater would be the restoring moment of the tail. So, a greater moment arm implies better stability and controllability.

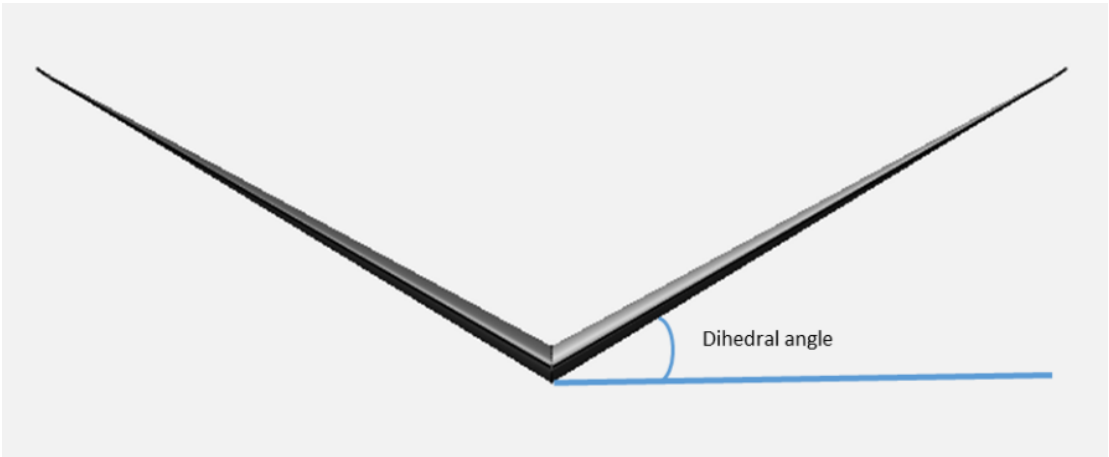

Figure 1.2: Representation of tail dihedral angle for lifting surfaces of the aircraft.

1.2 Literature Review

In the late 19th century men knew how to construct wings and glider airplanes. These glider airplanes when driven through air at sufficient speed, generated enough lift to sustain the weight of the wings and the person flying the glider. Wright brothers were the pioneers of aircraft industry. They made a lot of important contributions to this industry. Wright brothers were the first ones to design an aircraft that had sufficient strength to weight ratio, capable of sustaining a powered flight [10]. They designed and built a wind tunnel and a balance system to conduct aerodynamic tests. In 1903 the first flight of an unstable aircraft at Kitty Hawk was achieved by Wright Brothers. According to them an aircraft must have the following qualities

- Good Aerodynamics
- Good Structure
- Good Propulsion
- Good Stability

For adequate stability and controllability on any aircraft, tails are used. Tails are located at the aft most section of an aircraft. They act as stabilizers for the aircraft [10]. Whenever there is a disturbance, tails produce forces and moments to nullify the disturbance and bring the aircraft back to equilibrium position. However, tails contribute to the drag [6] and radar cross-section of the aircraft so they also have a negative impact on aircraft operation. The tails basically stabilize and control the dynamics of any aircraft about the longitudinal, lateral and vertical axes. The extent to which is governed by their position and geometry. There are different concepts of tail geometry. An aircraft can have T tails, V tails or Y tails etc. All of these tails have different extent of contribution towards stability of an aircraft.

While designing the tails of an aircraft only the static stability contribution is considered [14] whereas the tails effect both static and dynamic stability of an aircraft. Therefore there is no well-defined empirical relation available between tail characteristics (tail dihedral angle) and dynamic stability (damping ratio). So, there is a need to observe the effects of variation in tail characteristics on aircraft dynamic stability.

Lots of people are working in this domain. Some researchers have developed a complete flight dynamics model of an aircraft using different techniques. Some of them used analytical equations [2], some used numerical methods such as vortex lattice method [3] while some developed the model based on experimental (wind tunnel testing) results [12] etc.

In addition, there are numerous research papers available regarding analysis of V-tails for stall performance at different angles of attack and at combined angles of attack and sideslip [5]. Tail dihedral angle is the most important parameter that governs the performance of tails. Effects of tail dihedral angle on stability [1] and control of an aircraft have been observed [16]. In these papers the effect of tail dihedral angle on static stability have been observed [1]. However, there is no method available to directly compute the effect of tail dihedral on dynamic stability of the aircraft. Dynamic stability requirements are important considerations in any aircraft design and therefore, must be catered for in the initial design phase. For this a direct empirical method is required to link the effects of tail geometry (or tail dihedral) with dynamic stability.

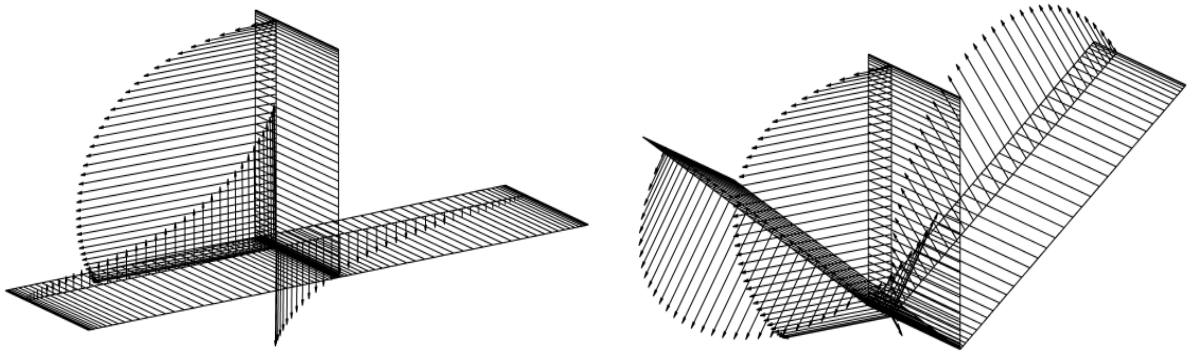

Figure 1.3: Lift distribution on a conventional tail (left) and on a tail with dihedral angle (right) [1]

The rest of this thesis consists of an introduction to different tail setups such as conventional tails, T-tails, inverted Y-tails, V-tails and inverted V-tails. Their contribution to drag and aerodynamic efficiency is discussed. Then the analytical models and method to achieve the required task are specified. In this section the software tools used are also described in detail. The next section is regarding the implementation of these methods using the software tools mentioned in the previous section. After this section the results obtained after applying the methods are discussed. In the last section the work is concluded and recommendations are given based on the results.

1.3 Tail Setups

Apart from a conventional tail setup, as shown in Fig 1.3, there are different tail arrangements that provide stability and controllability similar to the conventional tail, but with less planform area requirement. These tail arrangements produce less drag and the aerodynamic efficiency of the aircraft remains uncompromised. Phillips et al, have stated in [1] that by

varying the horizontal tail dihedral angle a particular empennage setup can provide better stability characteristics.

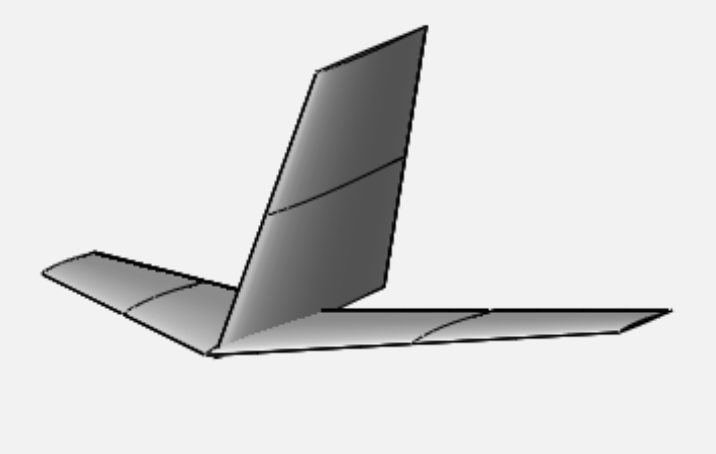

Figure 1.4: Conventional tail setup with a horizontal tail and a vertical tail.

In addition, the dihedral angle of the horizontal tail can be increased or decreased, consequently producing a completely different tail setup in both cases. These different tail setups provide different stability characteristics and have different area requirements [1].

As these tail setups are produced with different dihedral angles and number of surfaces, the aerodynamic interaction between these surfaces also vary [10]. Increasing the tail dihedral angle of the horizontal tail in a conventional tail setup, as illustrated in Fig 1.4, the aerodynamic interaction between the horizontal tail and the vertical tail will increase due to the reduced gap in between them [1].

This increase in aerodynamic interaction produces vortices and accounts for the loss of stability and controllability contribution of the empennage due to reduction in the effective tail area. Therefore, conventional tails tend to produce undesirable results when increasing the tail dihedral angle (Fig 1.4).

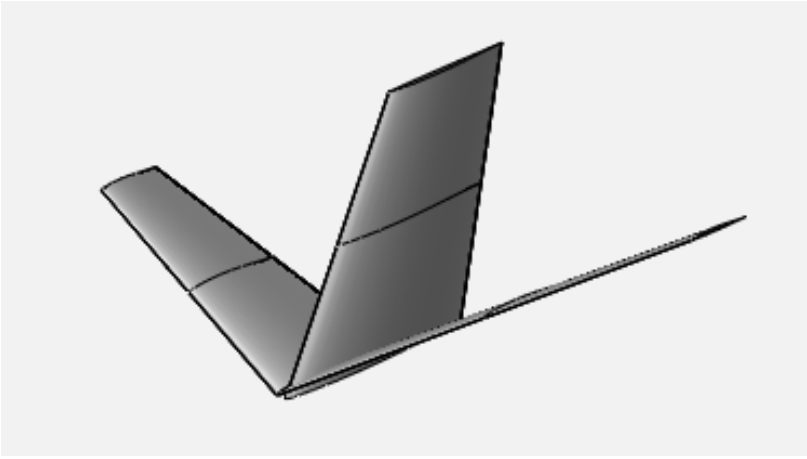

Figure 1.5: Conventional tail setup with 20 degrees dihedral angle to the horizontal tail.

In addition, the area requirement of the conventional tail setup is large. This tail setup is not suitable for aircraft with high stability requirements (Static Margin up to 15%) [5].

Considering a T-tail setup (Fig 1.5), better stability and controllability can be achieved by increasing the tail dihedral angle of the horizontal tail. [1]

By increasing the tail dihedral angle of the horizontal tail in a T-tail setup, the aerodynamic interactions between these surfaces do not increase due to the increase in gaps. Therefore, the loss in effective tail area does not occur.

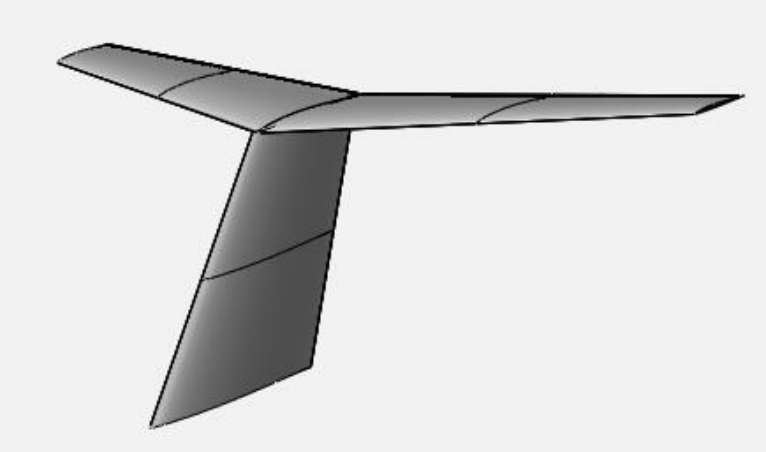

Figure 1.6: A T- tail setup. Horizontal tail installed at tip of vertical tail.

Furthermore, increasing the negative dihedral angle (anhedral) of the horizontal tail in a conventional tail setup also increases the gaps as it can be seen in Fig 1.6. This reduces aerodynamic interaction between the tails and the particular setup is called an inverted Y tail.

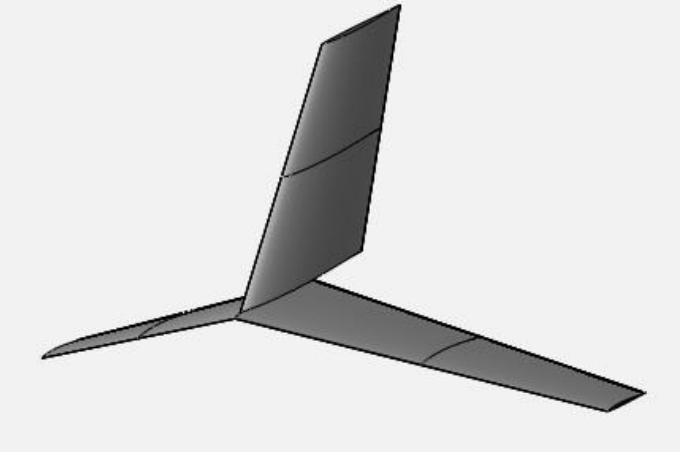

Figure 1.7: Inverted Y tail setup. It consists of a horizontal tail with anhedral angle, installed below the vertical tail.

By increasing tail dihedral angle, aircraft directional static stability increases due to an addition in vertically projected area of the tail. On the other hand, increasing tail dihedral reduces longitudinal static stability due to reduction in horizontally projected area of the tail. Therefore by increasing the tail dihedral angle the vertical tail area requirement reduces due

to additional vertical projection area. The horizontal tail dihedral angle can be increased in such a way as to completely eliminate the need of a vertical tail [4]. This particular tail setup is called a V-tail (Fig 1.7).

Figure 1.8: (a) Left: A V-tail setup with dihedral angle (b) Right: An inverted V-tail setup with anhedral angle.

All the tail setups mentioned above produce different stability characteristics and impact differently on the aerodynamic efficiency of the aircraft.

However, by increasing the horizontal tail dihedral angle, mounted at the root of the vertical stabilizer, causes the interference drag to increase due to reduced gap and increased vorticity between the respective surfaces. On the other hand, by increasing the horizontal tail dihedral angle, mounted at the tip of the vertical stabilizer, causes the interference drag to decrease due to increased gap and reduced vorticity between the respective surfaces.

In order to get the most suitable tail setup, a comparison of the stability contribution of these different tail setups with their impact on the aerodynamic efficiency of the aircraft must be performed.

1.4 Stability and Controllability

Stability can be defined as the tendency of an object to come back to its equilibrium state. Aircraft stability can be divided into two types, static stability and dynamic stability. Static stability is the initial tendency of an aircraft to return to its equilibrium position [10]. It is defined about all the axes (lateral, longitudinal and directional). If an aircraft is stable with respect to pitch then it is said to be statically longitudinally stable. Similarly if an aircraft is stable with respect to roll and yaw then it is said to be statically laterally and directionally stable respectively.

For an aircraft to be dynamically stable it is necessary that it must be statically stable. So, static stability is a prerequisite for dynamic stability. An aircraft can go into some

conventional longitudinal and lateral-directional modes due a particular disturbance in flight. These modes are given as follows

- Longitudinal
    - Short Period
    - Phugoid
- Lateral-Directional
    - Dutch Roll
    - Spiral
    - Roll Subsidence

Dynamic stability of an aircraft can be defined in terms of these conventional dynamic modes. If an aircraft is stable in these modes then it is dynamically stable. It should also be noticed here that lateral and directional dynamic modes are categorized under one category. This is due to coupling of roll and yaw dynamics of the aircraft during actual flight. Conventionally, an induced rolling motion from pilot command or external disturbance will cause the aircraft to yaw and vice versa. Therefore, roll and yaw dynamics are categorized as one.

Controllability is the ability of an aircraft to maneuver from one flight condition to another. In technical terms, it is the ability of the aircraft to trim at a particular angle of attack and sideslip angle. The larger the trim angle of attack and/or sideslip angle, the greater would be the controllability. In lateral axis, controllability is defined as the time taken for the aircraft to roll to a specific bank angle. Intuitively, smaller the time taken to roll for an aircraft the greater would be the controllability in lateral axis. Similarly in longitudinal and directional axis, controllability is defined as the time taken for the aircraft to pitch and yaw to a specific pitching and yawing angle respectively.

1.5 Tail Dihedral and Flying Qualities

Aircraft tail geometry can significantly impact its stability and controllability. Its influence on flight dynamics depends on a number of geometrical parameters such as planform area, longitudinal location, sweep angle and tail dihedral. These parameters also effect the aerodynamic performance of an aircraft. By increasing the planform area one can achieve better stability and controllability characteristics however, also compromise on the aerodynamic efficiency of the aircraft due to the increasing drag. Conventional T-tail setup as shown in Fig 1.8(a) consists of a horizontal stabilizer and a vertical stabilizer. These

stabilizers have their corresponding drag contribution due to the respective planform areas. An additional drag force is produced due to the aerodynamic interference in between these stabilizers. Therefore, the drag penalty of a conventional tail setup is significant.

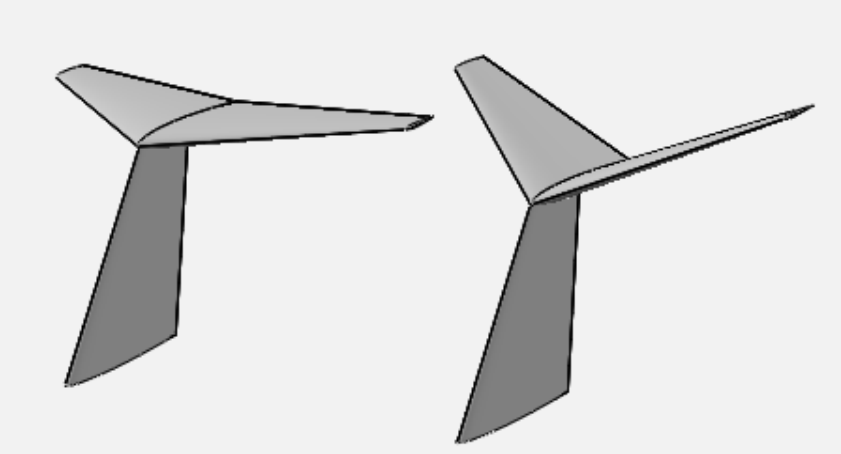

Figure 1.9: (a) Left: Conventional T-tail setup. (b) Right: Conventional T-tail setup with horizontal tail dihedral.

In order to increase the positive tail contribution to stability and controllability, a certain geometrical change is required which also improves aerodynamic efficiency. Tail dihedral is a geometrical parameter which can influence aircraft stability. By increasing tail dihedral aircraft directional static stability increases due to an addition in vertical projection area of the tail. On the other hand, increasing tail dihedral reduces longitudinal static stability due to reduction in horizontal projection area of the tail.

Dihedral angle of the horizontal tail can be selected in such a way to provide adequate static longitudinal stability and directional stability. A horizontal tail with dihedral angle provides better stability and control characteristics if it is mounted above the vertical tail [1]. This particular tail setup produces less interference drag as compared to a conventional T-tail setup [1].

However, by increasing the horizontal tail dihedral angle, mounted at the root of the vertical stabilizer, causes the interference drag to increase due to reduced gap and increased vorticity between the respective surfaces.

The dihedral angle also reduces the need of a large vertical stabilizer thus, reducing the drag contribution of the vertical stabilizer [1]. Therefore, a horizontal tail dihedral can provide directional and longitudinal stability and control simultaneously with the advantage of producing less drag as compared to conventional T-tail setup.

The dihedral angle of the horizontal tail reduces static longitudinal stability and increases static directional stability. Thus, increasing the dihedral angle has its advantages as well as

disadvantages. Therefore, it is a necessity to select the most optimal dihedral angle in tail design procedure in order to prevent the loss of static longitudinal stability below standard requirements.

It is essential for the aircraft tail setup (with or without dihedral angle) to provide sufficient dynamic longitudinal and lateral-directional stability in order to fulfill the requirements of aircraft flying qualities (MIL-F-8785C) mentioned in Table 1.1. These requirements are of longitudinal and lateral-directional dynamics in terms of their respective damping ratios.

Table 1.1: Aircraft flying qualities (MIL-F-8785C) [11]

	Longitudinal Damping Ratio	**Lateral-Directional Damping Ratio**
Level 1	0.35	0.08
Level 2	0.25	0.02
Level 3	0.15	0.00

This research work presents a method to select the most appropriate dihedral angle of horizontal tail to provide sufficient longitudinal and lateral-directional damping ratio in accordance to the flying qualities mentioned in Table 1.1. The method is based on mathematically modelling the change in longitudinal damping ratio and lateral-directional damping ratio with change in horizontal tail dihedral angle. The tail setup used in this research is a T-tail setup as the dihedral angle in this particular tail setup provides positive effects to aircraft aerodynamics (increased stability and reduced drag).

CHAPTER 2. ANALYTICAL MODELS AND NUMERICAL METHODOLOGY

The first step in the process is the selection of an aircraft geometry. For this purpose the geometrical dimensions of the aircraft selected should be available. A high subsonic executive aircraft Gulfstream G-550 was selected. The geometric parameters for the aircraft are available at the official website [22] of Gulfstream. These parameters (Appendix A) were used to generate a 3D model of the aircraft G-550.

2.1 Vehicle Sketch Pad (VSP)

VSP is a software used to generate a 3D model of aircraft and other vehicles. The geometric parameters of the aircraft to be modelled must be known. The model then generated using VSP can be processed into formats suitable for different engineering analysis tools. The 3D model for Gulfstream G-550 was generated using VSP.

2.2 Athena Vortex Lattice (AVL)

After generating a 3D model of Gulfstream G-550 the next step was to perform stability and control analysis on the geometry. Athena Vortex Lattice method was selected to perform simulations on the aircraft geometry. Athena is an open source software developed by Mark Drela, a professor of Fluid Dynamics at Massechusetts Institute of Technology (MIT) and an elected member of American Institute of Aeronautics and Astronautics (AIAA).

AVL is a program used for the aerodynamics and flight-dynamics analysis of rigid body aircraft of arbitrary configuration. AVL uses an extended vortex lattice method for the calculation of lifting surfaces (wings and tail group) and a slender body model for fuselage-like surfaces (fuselage and nacelles). The flight dynamic analysis combines a full linearization of the aerodynamic model about any flight state, together with specified mass properties [3].

The wing is modeled in the geometry record by deciding on the coordinates of the main edge of the preferred sections (modifications at the plan view of the wing, changes on airfoil geometry). The narrow frame model could be very constrained and the results may now not be as anticipated. Modeling using narrow bodies implies the cross-section to be round. The angles of attack should be low for the vortex lattice to work adequately. The drift is handled

as quasi-regular, in which the unsteady motion is adequately sluggish. The angular velocities additionally are required to be low, being restricted to the following limits,

$$-0.10 < \frac{pb}{2V} < 0.10$$

$$-0.03 < \frac{qc}{2V} < 0.03$$

$$-0.25 < \frac{rb}{2V} < 0.25$$

Where p, q and r are roll, pitch and yaw rates respectively. V is the aircraft velocity. b is wing span and c is wing mean aerodynamic chord [3]. The movement of the aircraft is actually very violent if any rate is outside these limits.

AVL applies a Prandtl-Glauert transformation to model compressibility due to high Mach number. An unswept wing can observe this variation at Mach numbers underneath 0.6 to ensure that the version works properly. At Mach 0.7, the model is prone to be incorrect due to the opportunity of transonic points, at Mach 0.8 it is totally unreliable and above Mach 0.8 it is completely inaccurate [3]. These limits are increased if swept wings are used.

2.3 Comparison of Tail setups

To perform a comparison in terms of stability and control of the aircraft, different tail setups were generated and incorporated on an aircraft model. A high subsonic speed executive jet was used for this purpose. A 3D CAD model was generated using the geometric parameters for a conventional executive aircraft. This geometry was then modified to get 3D models with different tail configurations. These geometries were incorporated into Athena Vortex Lattice method (AVL) environment [4].

Table 2.1: Different aircraft configurations and their respective tail setups.

Configuration	Tail Setup	Dihedral Angle (Degrees)
1	T-Tails	--
2	Inverted Y-Tails	-20
3	Inverted V-Tails	-27
4	V-Tails	27

The dihedral/anhedral angle of 27^{o} provides the best minimum area solution for a particular tail setup [1]. Therefore, the dihedral/anhedral angle of V-Tails and inverted V-Tails was

selected as 27°. The tail setup with dihedral/anhedral angle of 27° completely eliminates the need of vertical tail, therefore the anhedral angle for Inverted Y-Tails was reduced to 20° in order to reduce the vertical projection area and hence, incorporate a vertical tail.

Aerodynamic analysis via VLM was performed at a high subsonic Mach of 0.8 and at an altitude of 41000 feet. Stability and control derivatives obtained by performing the aerodynamic analysis, for different tail setups were recorded and analyzed.

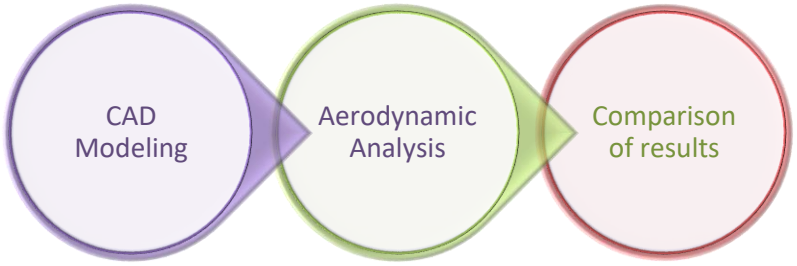

Figure 2.1: A schematic flow diagram for comparison of different tail setups.

2.4 T-Tails with varying dihedral angle

The 3D CAD model in which T-Tails were incorporated was altered by changing the tail dihedral angle and multiple CAD models were generated with different dihedral angles of horizontal tail.

Table 2.2: Different tail configurations and their respective dihedral angles.

Configuration	Tail Dihedral (degrees)
1	0
2	10
3	20
4	30
5	40

These geometries were imported into AVL environment. Aerodynamic analysis via AVL was performed again at 0.8 Mach and at an altitude of 41000 feet. Stability derivatives obtained

from this particular aerodynamic analysis, for different tail configurations were recorded and analyzed.

These derivatives were plugged in state space matrices to form a complete state space system and its corresponding eigen values. The eigen values for longitudinal and lateral-directional dynamics were distinguished and were used to compute the damping ratio of respective dynamic modes.

The damping ratios for longitudinal and lateral-directional motion against different tail configurations were compared. Plots were generated for different longitudinal and lateral-directional damping ratios against all tail configurations. This data obtained from preliminary analysis was used to obtain a relation between the damping ratio of longitudinal and lateral-directional modes with tail dihedral angle. This relation was obtained using curve fitting technique in MATLAB.

Using aircraft handling qualities mentioned in Table 1.1, an acceptable range of damping ratio for longitudinal and lateral-directional motion was obtained for Level 1 flying quality. This particular range of longitudinal and lateral-directional damping ratio was mapped onto the mathematical model between tail dihedral angle and damping ratio to obtain the lower and upper bound for the tail dihedral angle. Any value of tail dihedral angle in between these bounds would provide sufficient longitudinal and directional stability to meet the requirements of aircraft flying qualities.

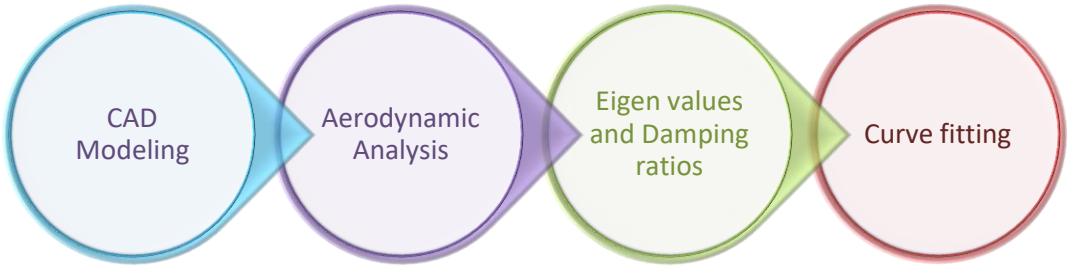

Figure 2.2: A schematic flow diagram to get optimum tail dihedral angle.

CHAPTER 3. IMPLEMENTATION

3.1 Aerodynamic Analysis

Aerodynamic analysis of the 3D models generated was performed using an extended vortex lattice method software. Geometrical parameters, mass properties and flight conditions of a high subsonic executive jet were imported into AVL environment using a series of input files. Fig 3.1 represents a 3D model of an executive jet with default T-tail setup and the same geometry generated by AVL using panel distribution method. The 3D CAD model was generated using Vehicle Sketch Pad (VSP).

Fig 3.2 shows the same aircraft geometry with V-Tail setup generated by AVL. As it can be seen from the figure this geometry does not include a conventional vertical tail.

The executive jet used in the analysis have particular stability requirements. These requirements can classify the executive jet as a stable aircraft about longitudinal and directional axes. The T-Tail setup used as a default configuration has particular tail volume coefficients. The stability and controllability of an aircraft is characterized by these tail volume coefficients. These volume coefficients are different for vertical and horizontal tail and are defined as follows,

$$C_{HT} = \frac{S_{HT} L_{HT}}{S_W \bar{c}_w}$$

$$C_{VT} = \frac{S_{VT} L_{VT}}{S_W b_w}$$

Where C_{HT} and C_{VT} are the horizontal and vertical tail volume coefficients respectively. S_{HT} and S_{VT} are horizontal and vertical tail planform areas. L_{HT} and L_{VT} are the horizontal and vertical tail moments arms respectively. b_w is wing span and $\bar{c}_w$ is the wing mean aerodynamic chord [23].

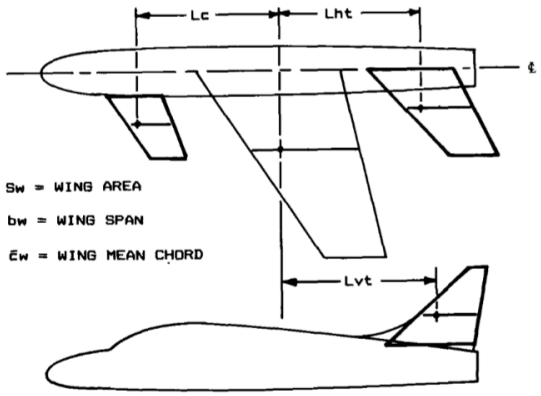

Figure 3.1: Definition of L_{HT} and L_{VT} in aircraft geometry [23].

The tail volume coefficients that fulfill the stability requirements of the default configuration are given in the Table 3.1.

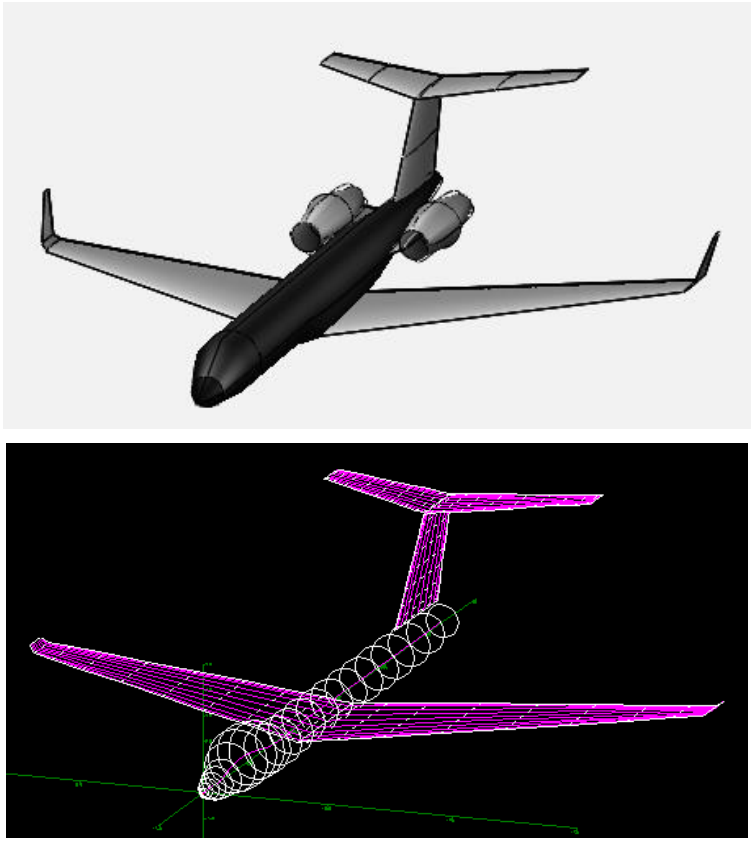

Figure 3.2. The 3D CAD model of the executive jet (above).

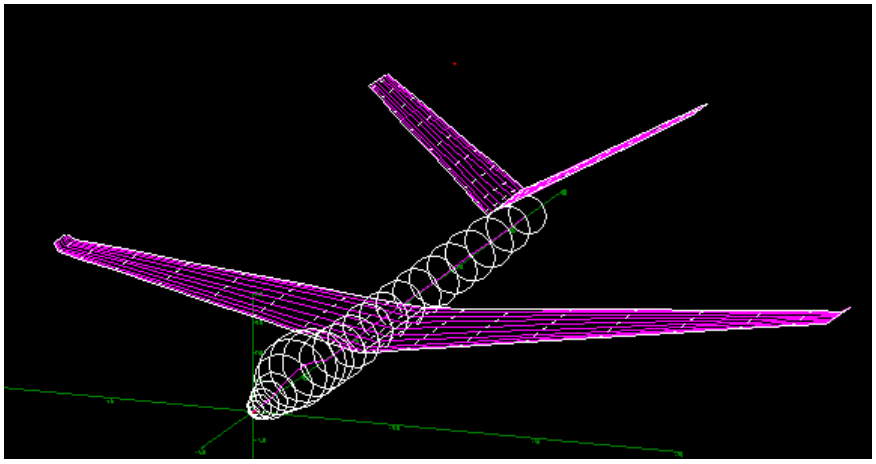

Figure 3.3. VLM panels generated by AVL for V-Tail setup.

Table 3.1: Tail volume coefficients for default configuration.

Volume Coefficient	**Value**
C_{VT}	0.0452
C_{HT}	1.4528

3.2 Stability Analysis

The 3D CAD model generated by using T-Tails as empennage of G-550, was altered by changing the tail dihedral angle and multiple CAD models were generated with different dihedral angles of horizontal tail.

The mass properties and flight conditions were also used as inputs. An empty weight of 21,909 kg was fed to Athena. Cruise flight condition was used at 0.8 Mach and at an altitude of 41,000 feet.

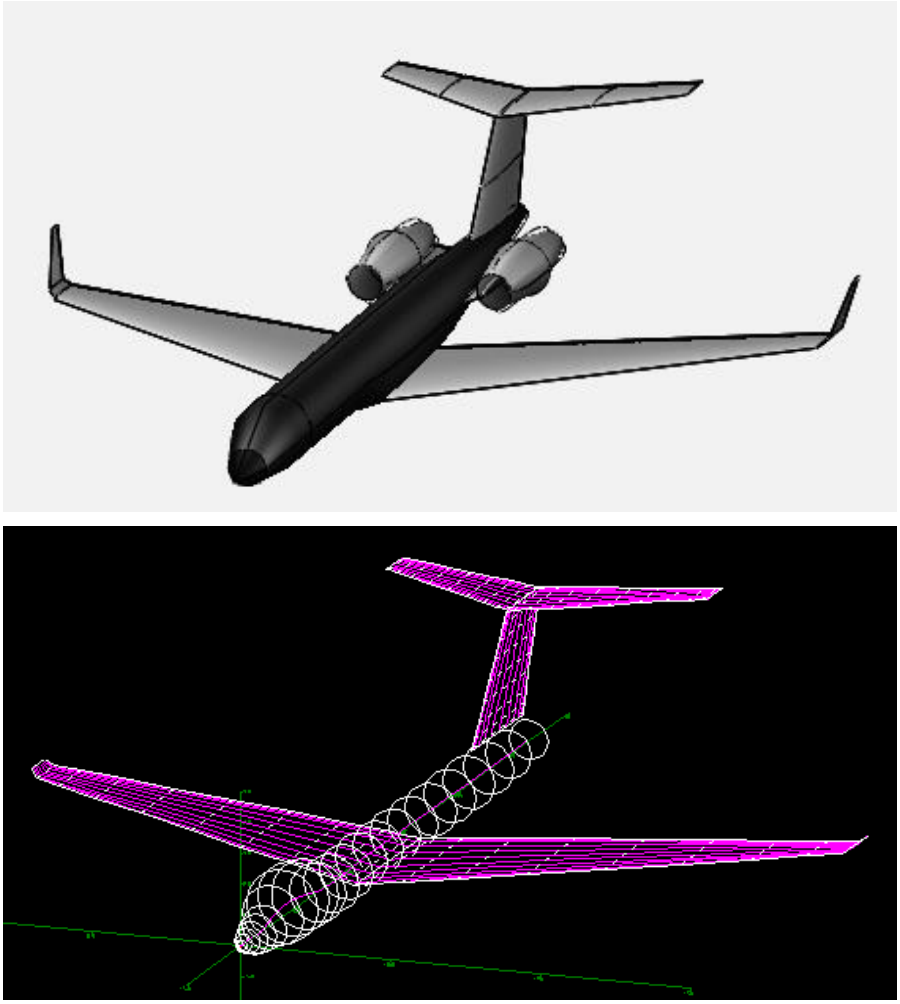

Figure 3.4: The 3D CAD model of the executive jet (above). Geometry generated by AVL for the executive jet using panel distribution (below).

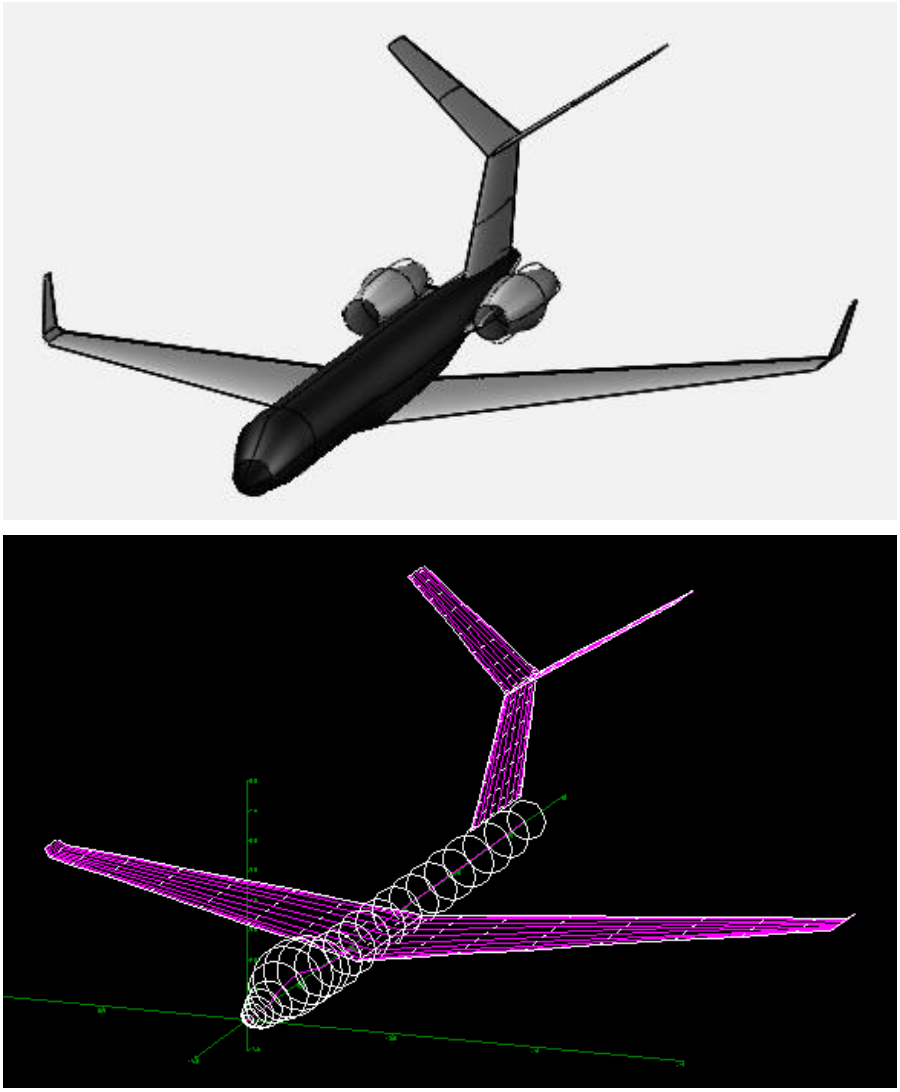

Figure 3.5: 3D CAD model (above) and VLM panels generated by AVL (below) for tail dihedral angle of 30 degrees.

Aerodynamic and stability coefficients obtained from AVL were recorded. These coefficients were recorded for all tail configurations mentioned in Chapter 4.

3.3 State Space System

The coefficients were plugged into the state space matrices to form a complete state space system. The state space system captured both longitudinal and lateral-directional dynamics of the aircraft. Thus, the matrices were used to compute longitudinal and lateral-directional eigen values using MATLAB. Subsequently, these eigen values were used to compute damping ratio of the respective dynamic modes using equation (1) and (2) [10].

$$\lambda = \eta \pm i\omega \qquad (1)$$

$$\zeta = \cos(tan^{-1}\left(\frac{\omega}{\eta}\right)) \qquad (2)$$

Where, η is the real part of the eigen value and ω is the imaginary part of the eigen value [10]. The longitudinal and lateral-directional damping ratios were recorded against each tail dihedral configuration. The data generated was transformed into mathematical equations, for longitudinal and lateral-directional damping ratios, using curve fitting technique in MATLAB (Appendix B).

3.4 Curve Fitting

For the most accurate curve fitting, different techniques were used to generate appropriate polynomial curves of different degrees. The R^2 value was calculated for each curve fitted onto the data. This value for each polynomial fit was compared.

The table below shows minimal error when 3rd degree (or higher) polynomial is selected for curve fitting. Therefore, a 3rd order polynomial was selected as the most suitable polynomial for curve fitting technique on longitudinal and lateral-directional damping ratios.

Table 3.2: Comparison of the r square value for different polynomials used for curve fitting of longitudinal and lateral-directional damping ratios.

Polynomial	**R^2 (ζ_{LONG})**	**R^2 (ζ_{LAT})**
Linear	0.8986	0.9395
2nd Degree	0.9574	0.9969
3rd Degree	0.9684	0.9998
4th Degree	0.9998	0.9998

After generating two different mathematical relations between longitudinal damping ratio, lateral-directional damping ratio and tail dihedral angle, the lower and upper bound of damping ratio was selected in accordance to the flying qualities in Table 1.1. From these limits of damping ratios, the lower and upper bound of the tail dihedral angle was determined. Any tail dihedral angle beyond these limits would result in an unacceptable flying quality in either longitudinal or lateral-directional motion.

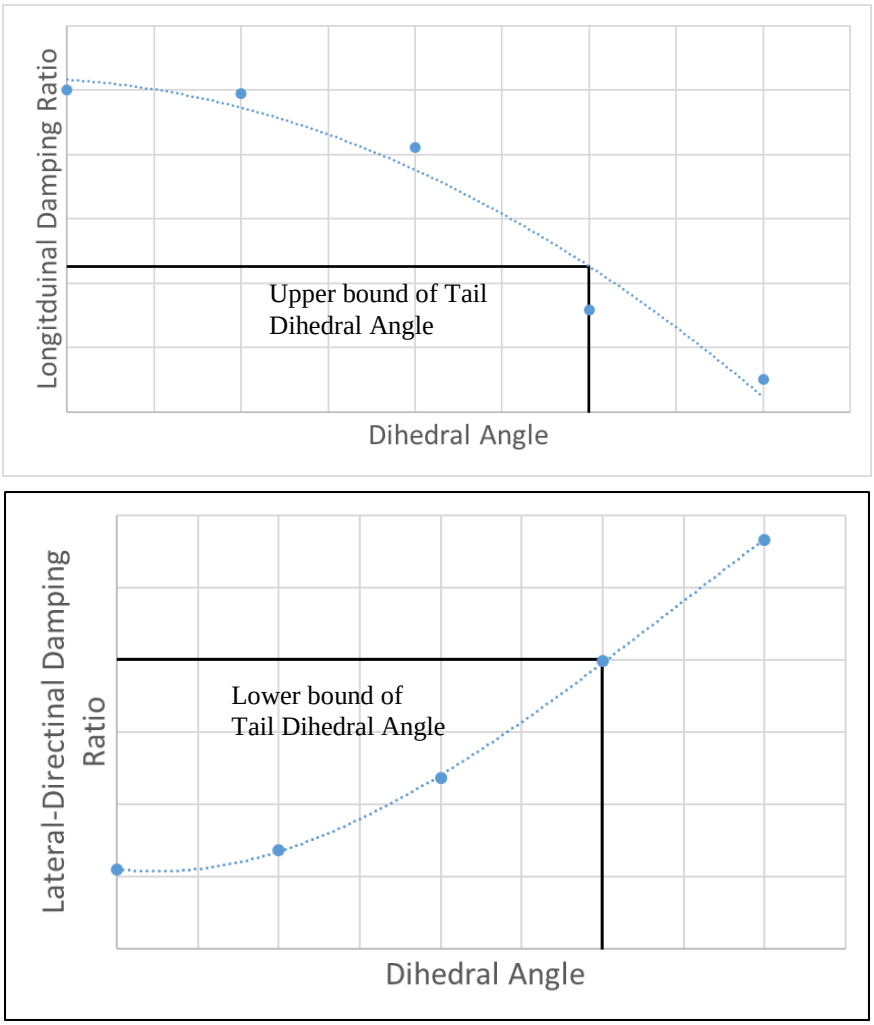

Figure 3.6: A schematic graphical representation of the upper (above) and lower bound of tail dihedral angle (below).

It can be observed from the Fig 3.5 that the lower bound of dihedral angle is governed by lateral-directional damping ratio limit. This is due to the reason that by decreasing the tail dihedral angle the side projected area of the tail reduces, thus reducing the directional stability and the lateral-directional damping ratio. Similarly, the upper bound of dihedral angle is governed by longitudinal damping ratio limit as increasing the dihedral angle of the tail reduces the horizontal projection area of the tail and thus, reduced longitudinal stability and damping ratio.

The tail dihedral angle should be of any value in between the lower and the upper bounds. These bounds are governed by the aircraft flying qualities as mentioned in Table 1.1 and would always ensure adequate longitudinal and lateral-directional dynamic stability to meet the flying quality requirements.

CHAPTER 4. RESULTS AND DISCUSSION

As mentioned earlier, a number of aircraft geometries with different tail configurations were generated. The tail configurations incorporated in the aircraft include inverted Y-tails, Inverted V-Tails and V-Tails setup. As the stability and control characteristics of an aircraft are governed by its tail volume coefficients. Therefore, these geometries were generated by keeping constant tail volume coefficients as the default configuration. The required tail size for different tail setups in order to achieve similar control volume coefficients was recorded and compared.

4.1 Static Stability Derivatives

The static stability derivatives [2] were obtained and compared for different tail setups. It can be seen from the Table 4.1 that the default configuration is stable about longitudinal axis and neutrally stable about directional and lateral axes.

Table 4.1: Static stability derivatives for all tail setups in per radian.

Tail Setup	$C_{m\alpha}$	$C_{n\beta}$	$C_{l\beta}$
T-Tails	-0.05003	0.000239	-0.00073
Inverted Y-Tails	-0.02474	0.001009	-0.00002
Inverted V-Tails	-0.04126	0.000036	0.00022
V-Tails	-0.04394	0.000208	-0.00115

From the table above it can be observed that with similar tail volume coefficients, T-Tails exhibit the highest static longitudinal stability. This is due to the fact that a complete horizontal tail is present in this particular tail setup and has the highest stable contribution to static longitudinal stability.

Inverted V-Tails and V-Tails provide approximately equal static longitudinal stability however the difference is due to the variation in aerodynamic interaction between the tail surfaces. Inverted V-Tails are installed below the fuselage line and experience vortices produced by the fuselage. These vortices are produced due to vortex breakdown at the tail end of the fuselage where the airflow above and below the fuselage meet. Therefore, these interactions account for the effective tail area loss in Inverted V-Tails hence, reducing their contribution to static longitudinal stability by 6%.

Similarly, this vortex break down effects the static directional stability contribution of the Inverted V-Tails to a much larger extent. The vertical projection of the inverted V-Tails is less due to low dihedral angle of 27 degrees. In addition, the vortex break down at the fuselage end reduces the effective area of the tail hence reducing the vertical projection by a larger extent. This reduction in effective vertical projected area reduces the static directional stability contribution of the inverted V-Tails by 82% as compared to the V-Tails.

Furthermore, inverted Y-Tails exhibits a highly stable contribution to static directional stability. This contribution is more than that of the default T-Tails setup. Inverted Y-Tails include a vertical tail, in addition, the vertical projection of the horizontal tail due to its anhedral angle increases the effective vertically projected area. Therefore, Inverted Y-Tails have a larger vertically projected area as compared to other tail setups and hence, a more stable static directional stability contribution.

From Table 4.1 it can also be observed that the V-Tails setup provide the highest static lateral stability. This contribution is 36% higher than that of the default T-Tails setup. The empennage provides its static lateral stability contribution from its vertically projected area. Aerodynamic interactions between the vertical and horizontal tail of a T-Tail setup reduces the effective area of the vertical tail hence, reducing the contribution of the vertical tail to static lateral stability.

However, it can also be observed from Table 4.1 that the T-Tail setup provides more stable contribution to static directional stability as compared to V-Tails setup. This is due the loss of effective vertically projected area in a V-Tail setup in pure sideslip. In pure sideslip motion the V-Tail root produces vorticity and therefore accounts for the loss of effective vertically projected area [1]. This reduction in vertically projected area reduces the static directional stability contribution of the V-Tails by 13% as compared to T-Tails.

Inverted V-Tails have an unstable contribution to static lateral stability due to the anhedral angle. Inverted Y-Tails provide a stable contribution to static lateral stability due to presence of the vertical tail. However, this stable contribution is approximately cancelled out by the unstable contribution due to the anhedral angle of the horizontal tail.

4.2 Control Derivatives

Along with stability, maneuverability also plays an important role in aircraft handling. Maneuverability of any aircraft is governed by its stability characteristics and control powers of the control surfaces. Increasing stability decreases maneuverability of the aircraft, whereas,

by increasing the control powers of the control surfaces, maneuverability can be increased. The control powers depend on the size, moment arm and arrangement of the control surfaces. The table below records the longitudinal and directional control powers of each tail setup used in the analysis.

Table 4.2: Longitudinal and Directional control powers for all tail setups.

Tail Setup	$C_{m\delta e}$	$C_{n\delta r}$
T-Tails	-0.06914	-0.00105
Inverted Y-Tails	-0.05381	0.00112
Inverted V-Tails	-0.07727	-0.00152
V-Tails	-0.07727	-0.00155

From Table 4.2, it can be observed that Inverted V-Tails and V-Tails have the most longitudinal control power. The longitudinal control power of Inverted V-Tails and V-Tails is 11% more as compared to the longitudinal control power of default T-Tails setup.

In addition, the directional control power of Inverted V-Tails and V-Tails is also more than that of T-Tails. The increase in directional control power is 27% in case of V-Tails and Inverted V-Tails.

This increase in directional and longitudinal control power for V-Tails and Inverted V-Tails is due to less interference caused by control deflection. V-Tails and Inverted V-Tails consist of two surfaces whereas, T-Tails consist of three surfaces. The larger number of surfaces in T-Tails increases aerodynamic interactions between these surfaces during control deflection. Hence, T-Tails render less control power as compared to V-Tails or Inverted V-Tails. Inverted Y-Tails produce the least control power in both longitudinal and directional axes due to high aerodynamic interactions between the surfaces and the fuselage.

4.3 Aerodynamic Efficiency

It is also important to measure the effect of different tail setups on the aerodynamic efficiency of the aircraft. This efficiency depends on the drag force produced by a particular empennage. The drag force of any surface or a body is dependent on its total wetted area [10]. Therefore, the total wetted areas of each tail setup are recorded below.

Table 4.3: Total wetted area of all tail setups.

Tail Setup	Total Wetted Area
T-Tails	77.65
Inverted Y-Tails	71.12
Inverted V-Tails	67.28
V-Tails	67.28

It can be observed from Table 4.3 that, V-Tails give the best stability and maneuverability characteristics with the lowest total wetted area. The reduction in wetted area is approximately 14% in the case of V-Tails. Thus, the V-Tails setup produce less drag and increases aerodynamic efficiency of the aircraft as compared to the default T-Tails setup. Thus, the V-Tails setup is the most suitable of all the tail setups.

4.4 Effect of varying Tail Dihedral

The impact of changing tail dihedral was recorded in terms of changes in longitudinal and directional static stability. In addition, the change in dynamic response (damping ratio) of the aircraft about longitudinal and lateral-directional axes was also recorded.

Fig 4.1 shows the change in static longitudinal and directional stability with change in tail dihedral angle. It can be observed that the static directional stability increases with increase in tail dihedral angle.

This is due to increase in the vertical area projection of the tail. On the other hand, static longitudinal stability decreases with increase in tail dihedral angle due to decrease in horizontal projection area of the tail. This reduction in horizontal projection area reduces the lifting force and consequently reduces the pitching moment.

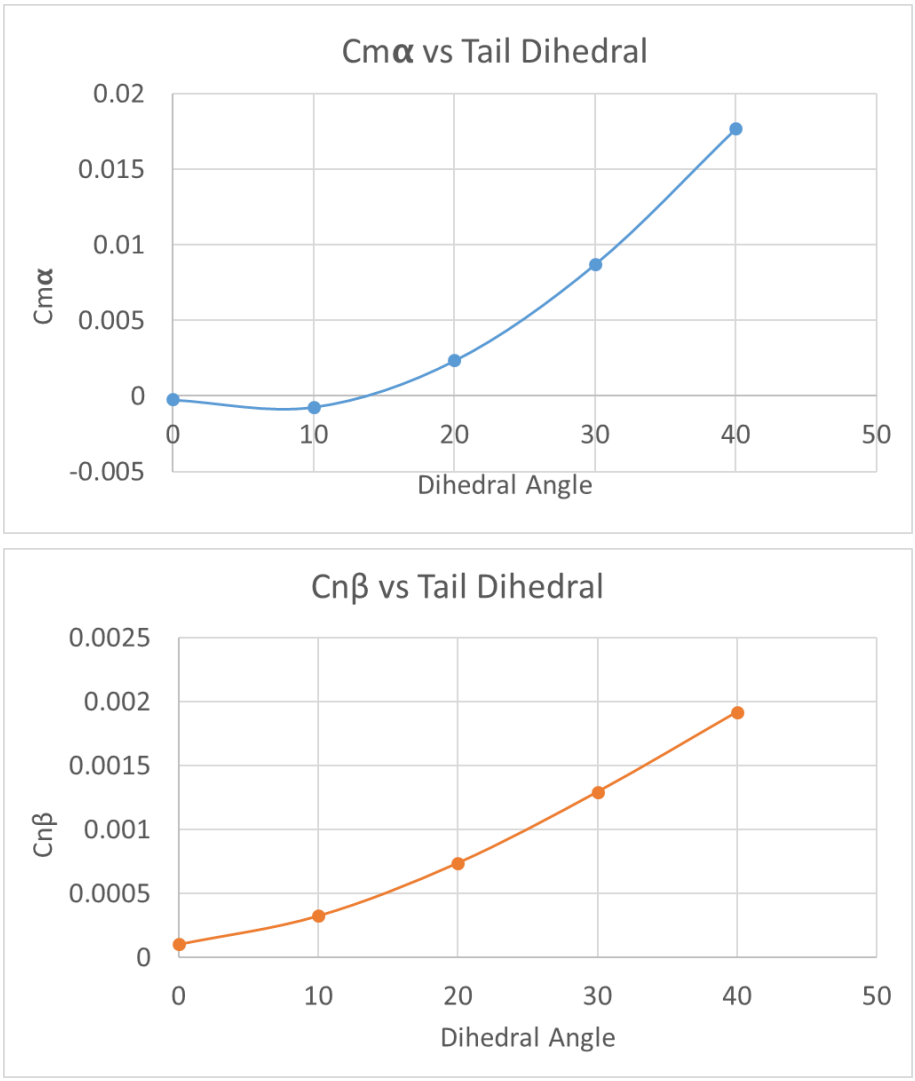

Figure 4.1: Plots for change in $C_{m\alpha}$ (above) and $C_{n\beta}$ (below) derivatives with respect to tail dihedral angle.

Table 4.4: Change in coefficient of lift and coefficient of pitching moment, at zero angle of attack, with tail dihedral angle.

Tail Dihedral (Degrees)	**C_m**	**C_L**
0	0.0828	-0.0156
10	0.0756	-0.0144
20	0.0658	-0.0126
30	0.0544	-0.0104
40	0.0426	-0.0082

Change in static longitudinal stability for tail dihedral angle of 10 degrees is minimum due to a very small change in lifting force and pitching moment generated by the tail. Table 4.4 records the coefficients of the lifting force and pitching moment generated by the tail at zero angle of attack. It can be observed that the change in these coefficients also increase with the increase in tail dihedral angle.

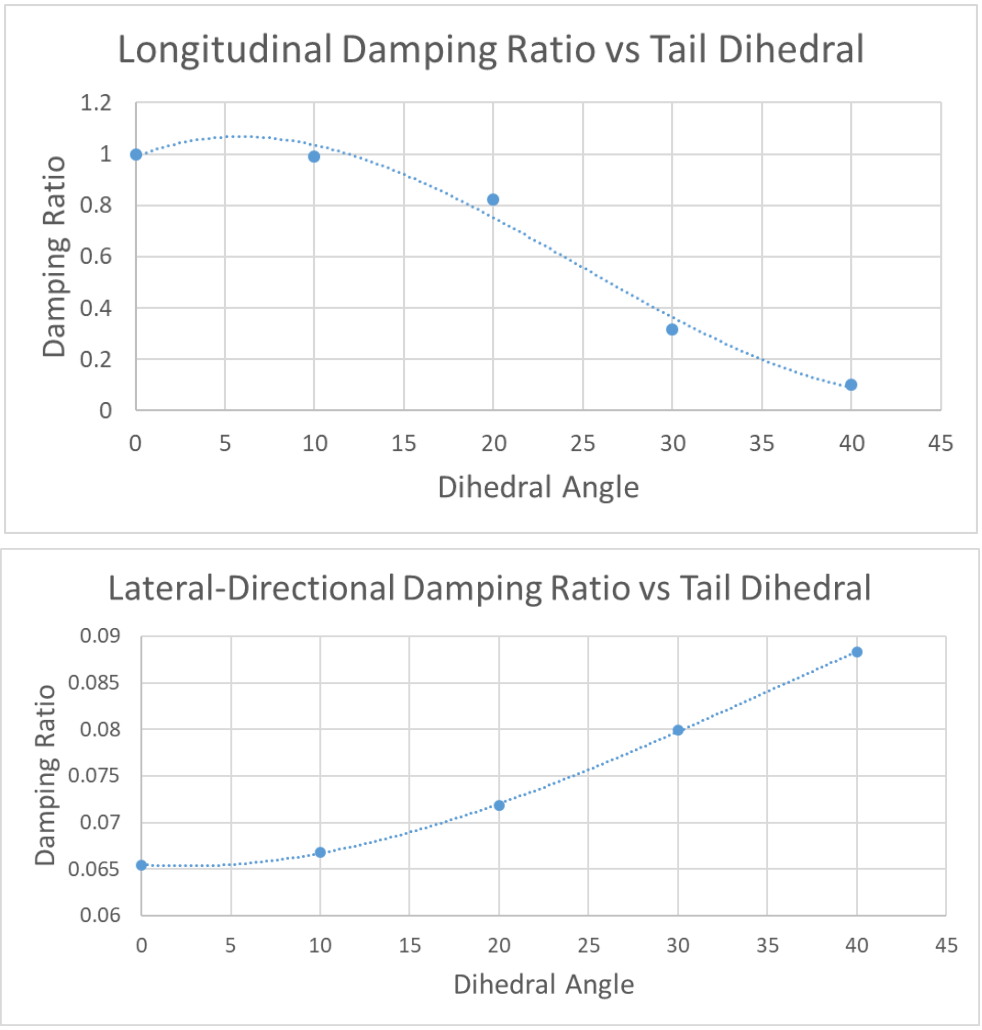

Figure 4.2: Change in longitudinal (above) and lateral-directional (below) damping ratios with tail dihedral angle.

Dynamic stability is represented in the form of different dynamic modes for longitudinal and lateral-directional axes. The damping ratios corresponding to these modes were recorded and plotted against tail dihedral angle.

Fig 4.2 shows change in longitudinal and lateral-directional damping ratios with tail dihedral angle. It can be observed that longitudinal damping ratio decreases by increasing tail dihedral angle whereas lateral-directional damping ratio increases by increasing tail dihedral angle. The increment of lateral-directional damping ratio is due to the increase in vertical projection area of the tail (with increasing tail dihedral angle) and thus, increase in the directional

stability of the aircraft. The decrement of longitudinal damping ratio is due to the decrease in horizontal projection area with increasing tail dihedral angle.

4.5 Mathematical Modelling

The data obtained for longitudinal and lateral-directional damping ratio was used to predict a suitable equation via curve fitting method. For the most accurate curve fitting, different techniques were used to generate appropriate polynomial curves of different degrees. The regression coefficient (R^2) value was calculated for each curve fitted onto the data. This value for each polynomial fit was compared.

The table below shows minimal error when 3rd degree (or higher) polynomial is selected for curve fitting. Therefore, a 3rd order polynomial was selected for curve fitting technique on longitudinal and lateral-directional damping ratios.

Table 4.5: Comparison of the r square value for different polynomials used for curve fitting of longitudinal and lateral-directional damping ratios.

Polynomial	**R^2 (ζ_{LONG})**	**R^2 (ζ_{LAT})**
Linear	0.8986	0.9395
2nd Degree	0.9574	0.9969
3rd Degree	0.9684	0.9998
4th Degree	0.9998	0.9998

The mathematical equations for longitudinal and lateral-directional damping ratios computed using curve fitting techniques are as follows:

$$\zeta_{\text{LONG}} = 4 \times 10^{-5}\Gamma^3 - 0.0028\Gamma^2 + 0.0284\Gamma + 0.9885 \quad (3)$$

$$\zeta_{\text{LAT}} = -3 \times 10^{-7}\Gamma^3 + 3 \times 10^{-5}\Gamma^2 - 0.0001\Gamma + 0.0655 \quad (4)$$

Where ζ_{LONG} and ζ_{LAT} are the longitudinal and lateral-directional damping ratios respectively. Γ is the tail dihedral angle.

Using international standards which define handling qualities (Appendix C) [11] of an aircraft, damping ratio values for level 1 flying qualities were recorded for both longitudinal and lateral-directional modes. These values were then incorporated in equation (3) and (4) to calculate upper and lower bounds for tail dihedral angle. As mentioned earlier lower bound for tail dihedral angle was governed by lateral-directional damping ratio limit while the upper

bound for tail dihedral angle was governed by the longitudinal damping ratio limit. The tail dihedral angles found using these relations are as follows:

Table 4.6: Upper and lower bounds of tail dihedral angle obtained using mathematical model generated.

	Dihedral angle (degrees)
Upper bound	31.6751
Lower bound	28.4172

Table 4.6 records the upper and lower bounds of tail dihedral angle that ensures Level 1 flying qualities of longitudinal and lateral-directional dynamics. The tail dihedral angle should lie within these bounds.

4.6 Mutable Flight Dynamics

Aerodynamics of the aircraft changes with change in flight speed and Mach number. This change also effects the flight dynamics and subsequently the longitudinal and lateral-directional damping ratios. In order to test the mathematical model obtained at high subsonic Mach number of 0.8, numerical analysis was performed for the same executive jet at low subsonic Mach numbers of 0.3 and 0.5 with different tail dihedral angles.

Table 4.7: Longitudinal and lateral-directional damping ratios recorded at low subsonic Mach numbers for the same aircraft model.

Mach No.	**Dihedral (degrees)**	**Axis**	**ζ (Numerical)**	**ζ (Model)**
0.3	10	Longitudinal	0.6899	0.9925
		Lateral-Directional	-0.0761	0.0672
	20	Longitudinal	0.8187	0.7565
		Lateral-Directional	-0.0542	0.0731
0.5	10	Longitudinal	0.7486	0.9925
		Lateral-Directional	0.0048	0.0672
	20	Longitudinal	0.9398	0.7565
		Lateral-Directional	0.0204	0.0731

The damping ratios obtained at these two subsonic Mach numbers were recorded and compared with the damping ratios obtained using the mathematical model.

It can be observed from the table above that the same mathematical model generated at a high subsonic Mach number cannot be used for predicting damping ratios at low subsonic Mach numbers. At low subsonic Mach numbers there is a considerable difference between the longitudinal damping ratios obtained using the mathematical model and Athena VLM (numerical). In addition, the lateral-directional dynamics of the aircraft completely change at low subsonic Mach numbers, as presented in the table above and cannot be predicted using the mathematical model at high subsonic Mach numbers. The difference is due to a complete shift in aerodynamics of the aircraft. With change in Mach number the complete longitudinal and lateral-directional dynamics of the aircraft changes.

Table 4.8: Change in aerodynamic coefficients with change in flight Mach number.

Mach No.	**$C_{m\alpha}$ (per radian)**	**$C_{n\beta}$ (per radian)**	**$C_{l\beta}$ (per radian)**	**$X_{N.P}$**
0.3	-0.2701	0.0332	-0.0435	15.84
0.5	-0.2316	0.0310	-0.0456	15.82
0.8	-0.0411	0.0187	-0.0531	15.75

From Table 4.8 it can be observed that there is a significant change in the values of $C_{m\alpha}$, $C_{n\beta}$ and $C_{l\beta}$ from subsonic Mach number of 0.5 to 0.8. However, there is a very small change in these coefficients from Mach 0.3 to 0.5. Therefore, there is significant change in aircraft dynamics (damping ratios) as the aerodynamic behavior of the aircraft completely changes. As a result, the mathematical model can only be used to predict the damping ratios and subsequently the most suitable tail dihedral angle for a single aerodynamic model.

CHAPTER 5. CONCLUSION

Different tail setups were incorporated onto Gulfstream G-550 which included T-Tails, Y-Tails, V-Tails, inverted V-Tails and inverted Y-Tails. Aerodynamic analysis was performed on these different combinations of tails. These tail setups were then compared with one another. From the comparison it was concluded that V-Tails provide the best stability and controllability characteristics with highest aerodynamic efficiency. This is because it has the least wetted area. Therefore, this particular tail setup produces the least drag force as compared to other tail setups. This particular tail setup produces less stable contribution to static longitudinal and directional stability as compared to T-Tail setup. This is due to the vortex shedding at the root of V-Tails. However, the difference is small. Whereas, the longitudinal and directional control powers for V-Tails are more than that of the T-Tails due to less aerodynamic interaction between the surfaces during control deflection.

A number of models were generated by varying dihedral angle of the horizontal tail of Gulfstream G-550. Stability and Control analysis was performed on all the models. Using the results of the analysis a mathematical model was generated to get optimum dihedral angle. Furthermore, the mathematical model was compared against numerical analysis on low subsonic Mach numbers. It was observed that the mathematical model was not able to predict longitudinal and lateral-directional damping ratios correctly at low subsonic Mach numbers. This is due to the change in aerodynamic behavior of the aircraft as Mach number changes. Thus, the mathematical model was found to be invalid for a different aerodynamic behavior. Therefore, it can also be concluded that the mathematical model is invalid for a completely different aircraft at a high subsonic Mach number.

5.1 Recommendations

The mathematical models generated for longitudinal and lateral-directional damping ratios with tail dihedral angle was only valid for the specific aerodynamic model. The aerodynamic model depends on the flight regime (altitude and Mach number) and aircraft geometry. Thus the model becomes invalid for a different flight regime and a completely different aircraft.

A further breakdown of the generated mathematical model is recommended. Each coefficient in the equations of longitudinal and lateral-directional damping ratios (equations 3 and 4) depends on specific parameters (aerodynamic, mass or geometrical). Therefore, it is necessary to find out those parameters that govern the values of these coefficients and thus the complete mathematical model.

APPENDIX A

Gulfstream G550 Parameters

GEOMETRY REPORT

	Wing	Stabiliser	Fin (excl.dorsal)	
Area, trapezoidal reference	1137.00	244.87	140.16	sq.feet
Area, piano gross	1141.15	244.87	140.16	sq.feet
Area, airbus gross	1132.11			sq.feet
Area, boeing wimpress	1137.00			sq.feet
Area, esdu	1137.00			sq.feet
Area, exposed	987.38	244.87	140.16	sq.feet
Area, wetted	2004.28	496.34	284.43	sq.feet
Aspect Ratio, trapezoidal	7.36	5.05	0.98	
Aspect Ratio, piano gross	7.34	5.05	0.98	
Aspect Ratio, airbus gross	7.39			
Aspect Ratio, boeing wimpress	7.36			
Aspect Ratio, esdu	7.36			
Span (excluding winglets)	91.50	35.16	11.72	feet
Sweepback at 1/4-chord	27.00	30.00	37.00	degrees
Taper Ratio (trapezoidal)	0.26	0.41	0.65	
t/c at root	0.100	0.090	0.095	
t/c at thickness break	n/a			
t/c at tip	0.083	0.090	0.095	

```
Volume Coefficient (V-bar)                0.612     0.041
Mean Aerodynamic Chord          13.86      7.37     12.14    feet
Arm between MAC 1/4 chords                39.36     30.26    feet

Wing chord at tip                                    5.13     feet
Wing chord at planform break                         n/a      feet
Wing chord at root (gross)                          18.48     feet
Wing chord at c/line (gross)                        20.78     feet
Wing chord at c/line (notional trapezoidal)         19.72     feet

Planform break location          0.000  (fraction of exposed semispan)
Thickness break location         0.000  (fraction of exposed semispan)

Wing location (station of extended leading edge at c/line):
33.90 feet    (39.5 % of fuse.length)

Spar locations (fractions of local trapez.chord):
Wing root: 0.08, 0.7       Wing tip: 0.14, 0.67

Fuel capacity  (avail/reqrd = 0.995)
-------------
(US.gal.: wing 4783.1, centre 1071.4, tail 0.0, adjust 309.5)

Total Available:  6164.00 US.gal. (geometric capacity)
Total Required :  6194.03 US.gal. (at mtow & design payload)

** WARNING: Fuel capacity shortfall is 30.03 US.gal.  **
```

Fuselage geometry

fuselage max. width	7.83	feet
fuselage max. depth	7.83	feet
length, total fuselage	85.83	feet
length, front section	14.61	feet
length, mid section	38.47	feet
length, rear section	32.74	feet
wetted area, total fuselage	1731.70	sq.feet
wetted area, front section	256.29	sq.feet
wetted area, mid section	945.99	sq.feet
wetted area, rear section	529.42	sq.feet

Nacelle geometry

nacelle length	16.24	feet
nacelle max. width	5.91	feet
nacelle max. depth	5.91	feet
wetted area per nac.	260.53	sq.feet

Overall dimensions

Span over winglets	93.50	feet
Overall aircraft length	96.38	feet
Height at top of fin	22.72	feet
Overall aircraft wetted area	5096.18	sq.feet

Gulfstream G550

PAYLOAD	8.	PAX = 1600.lb.
MTOW	91000.	lb.
OEW	48300.	lb. = 53.1% of mtow
FUEL-CAP.	6164.	US.gal. Avail/Req=1.00
SPAN	91.5	feet excl.winglets
WING-AREA	1137.	sq.feet trapezoidal
ENG.THRUST	16000.	*2 lbf. reference fn*
	15385.	*2 lbf. available slst
W/S	80.	p.s.f. trapezoidal
T/W	0.352	reference
	0.338	available

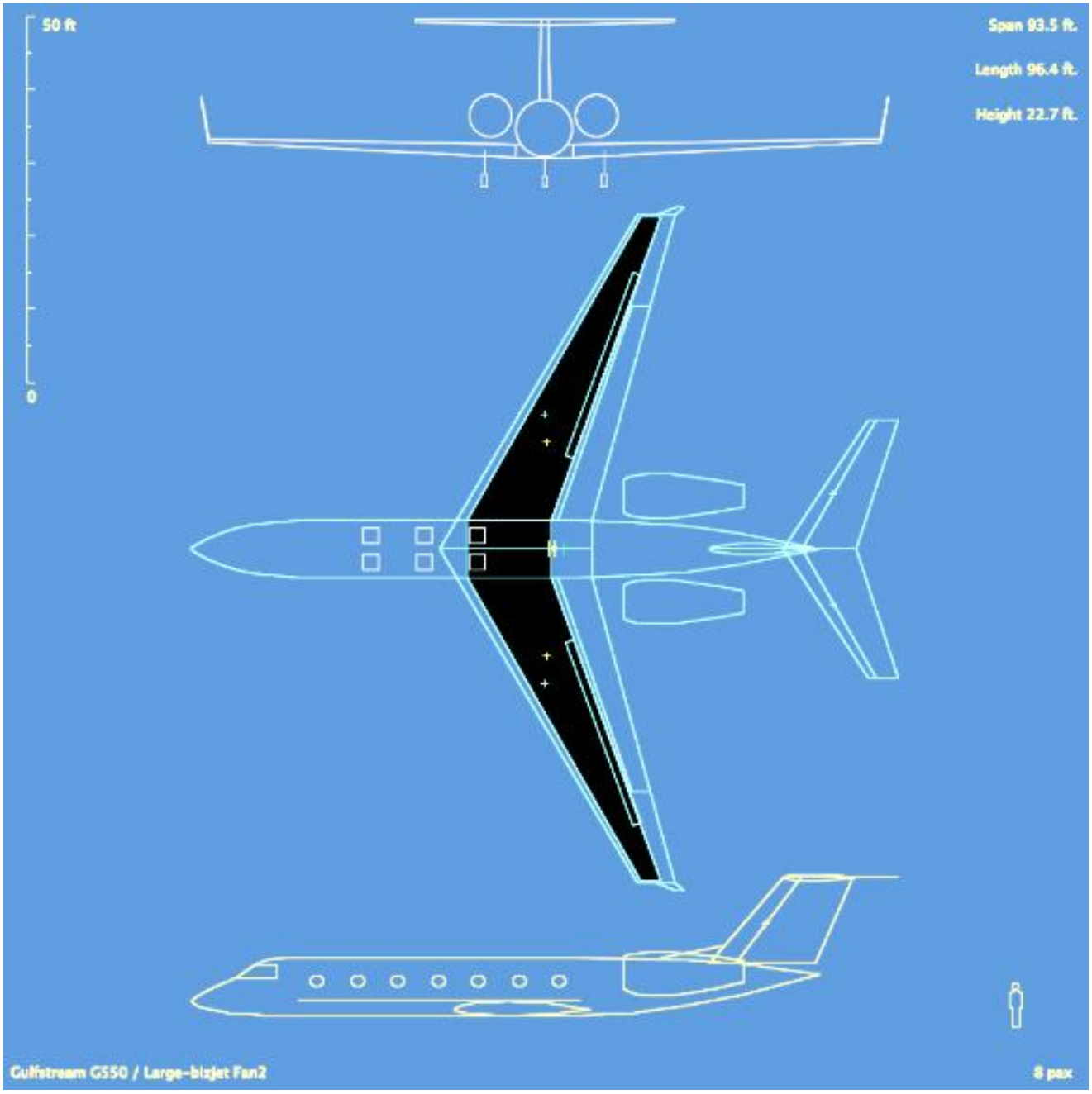
50 ft
0
Span 93.5 ft.
Length 96.4 ft.
Height 22.7 ft.
Gulfstream G550 / Large-bizjet Fan2
8 pax

APPENDIX B

MATLAB code for curve fitting

```
clc
clear all

%Longitudinal Dynamics
x = [0,10,20,30,40];
y = [1, 0.989026,   0.821557,   0.318474,   0.102404];
p = polyfit(x,y,3);
figure
plot(x,y)
hold on
plot(x,y,'o')
Dih = [4.00E-05 -0.0028 0.0284 0.6385];
%Dih = [-0.0005 -0.0033 0.8329];
y = roots(Dih)

%Lateral Dynamics
xl = [0,10,20,30,40];
yl = [0.065472, 0.066838,   0.071829,   0.079896,   0.088312];
pl = polyfit(xl,yl,3);
figure
plot(xl,yl)
hold on
plot(xl,yl,'o')
Dihl = [-3.00E-07 3.00E-05 -0.0001 -0.0145];
%Dihl = [1.00E-05 1.00E-04 -0.0148];
yl = roots(Dihl)
```

APPENDIX C

Flying Qualities MIL-F-8785C

Table 6.2 Definition of Flight Phase Categories

MIL–F–8785C	Suggested Civilian Equivalent: VLA, FAR 23 and FAR 25
Non–terminal Flight Phases	
Category A: Those non–terminal flight phases that require rapid maneuvering, precision tracking or precise flight path control. Included in this category are:	
a) Air–to–air combat (CO)	None
b) Ground attack (GA)	None
c) Weapon delivery/launch (WD)	None
d) Aerial recovery (AR)	None
e) Reconnaissance (RC)	Observation, Pipeline spotting and monitoring
f) In–flight refuelling (receiver) (RR)	None as yet
g) Terrain following (TF)	None
h) Anti–submarine search (AS)	Fish spotting
i) Close formation flying (FF)	Air–show demonstrations
Category B: Those non–terminal flight phases that are normally accomplished using gradual maneuvers and without precision tracking, although accurate flight–path control may be required. Included in this category are:	
a) Climb (CL)	Various climb segments
b) Cruise (CR)	Various cruise segments
c) Loiter (LO)	Flight in holding pattern
d) In–flight refuelling (tanker) (RT)	None as yet
e) Descent	Various descent segments
f) Emergency descent (ED)	Emergency descent
g) Emergency deceleration (DE)	None
h) Aerial delivery (AD)	Parachute drop
Category C: Terminal flight phases are normally accomplished using gradual maneuvers and usually require accurate flight path control. Included in this category are:	
a) Takeoff (TO)	Various takeoff segments
b) Catapult takeoff (CT)	None
c) Approach (PA)	Various approach segments
d) Wave–off / go–around (WO)	Aborted approach
e) Landing (L)	Various landing segments

Table 6.9 Short Period Damping Ratio Limits
MIL–F–8785C

Level	Category A and C Flight Phases Minimum	Maximum	Category B Flight Phases Minimum	Maximum
Level 1*	0.35 ← ζ_{sp} →	1.30	0.30 ← ζ_{sp} →	2.00
Level 2	0.25 ← ζ_{sp} →	2.00	0.20 ← ζ_{sp} →	2.00
Level 3	0.15** ← ζ_{sp} →	no maximum	0.15* ← ζ_{sp} →	no maximum

Table 6.7 Phugoid Damping Requirements

	MIL–F–8785C	VLA, FAR 23 and FAR 25
Level I:	$\zeta_{ph} \geq 0.04$	No requirement
Level II:	$\zeta_{ph} \geq 0$	No requirement
Level III:	$T_{2_{ph}} \geq 55$ sec	No requirement

Table 6.14 Maximum Allowable Roll Mode Time Constant
MIL–F–8785C

Flight Phase Category	Airplane Class	Level 1	Level 2	Level 3
A	I and IV	$T_r \leq 1.0$ sec	$T_r \leq 1.4$ sec	$T_r \leq 10.0$ sec
	II and III	$T_r \leq 1.4$ sec	$T_r \leq 3.0$ sec	$T_r \leq 10.0$ sec
B	All	$T_r \leq 1.4$ sec	$T_r \leq 3.0$ sec	$T_r \leq 10.0$ sec
C	I, II–C and IV	$T_r \leq 1.0$ sec	$T_r \leq 1.4$ sec	$T_r \leq 10.0$ sec
	II–L and III	$T_r \leq 1.4$ sec	$T_r \leq 3.0$ sec	$T_r \leq 10.0$ sec

Table 6.13 Minimum Time to Double the Amplitude in the Spiral Mode
MIL–F–8785C

Flight Phase Category	Level 1	Level 2	Level 3
A and C	$T_{2_s} > 12$ sec	$T_{2_s} > 8$ sec	$T_{2_s} > 4$ sec
B	$T_{2_s} > 20$ sec	$T_{2_s} > 8$ sec	$T_{2_s} > 4$ sec

Table 6.12 Minimum Dutch Roll Undamped Natural Frequency and Damping Ratio Requirements

Mil-F-8785C

Level	Flight Phase Category	Airplane Class	Min. ζ_d *	Min. $\zeta_d\omega_{n_d}$ * rad/sec	Min. ω_{n_d} rad/sec
Level 1	A (Combat and Ground Attack)	IV	0.4	-	1.0
	A (Other)	I and IV	0.19	0.35	1.0
		II and III	0.19	0.35	0.4**
	B	All	0.08	0.15	0.4**
	C	I, II-C and IV	0.08	0.15	1.0
		II-L and III	0.08	0.10	0.4**
Level 2	All	All	0.02	0.05	0.4**
Level 3	All	All	0	-	0.4**

REFERENCES

[1] W. F. Phillips, A. B. Hansen and W. M. Nelson, "Effects of Tail Dihedral on static stability," JOURNAL OF AIRCRAFT, vol. 43, pp. 1829-1837, 2006.

[2] Swati Swankar, Hardik Parwana, Mangal Kothari and Abishek, "Development of Flight Dynamics model and control of Biplane-quadrotor UAV," in AIAA Guidance, Navigation and Control Conference, Kissimmee, Florida, 12 January 2018.

[3] Mark Drela and Harold Youngren, "AVl doc," MIT Aero & Astro Harold Youngren, Aerocraft, Inc., 12 February 2017.

[4] j. A. Kidd, "Investigation of the Effect of Variable Tail Dihedral on Airplane Stability and Control," in AIAA, Aug 1998.

[5] M. J. Abzug, "V-Tail Stalling at Combined Angles of Attack and Sideslip," Journal of Aircraft, vol. 36, 1999.

[6] W. F. Phillips and D. O. Synder, "Modern Adaptation of Prandtl's ClassicLifting-LineTheory," Journal of Aircraft," AIAA, pp. 662-670, 2000.

[7] W. F. Phillips, N. R. Alley and W. D. Goodrich, "Lifting-Line Analysis of Roll Control and Variable Twist," Journal of Aircraft, vol. 41, pp. 1169-1176, 2004.

[8] W. F. Phillips, "Lifting-Line Analysis for Twisted Wings and Washout-Optimized Wings," Journal of Aircraft, vol. 41, pp. 128-136, 2004.

[9] R. L. Baren Johnson, "Characterizing Wing Rock as a Function of Size and Configuration of Vertical Tail," in Flight Mechanics Conference, Chicago, Illinois, 2009.

[10] R. C. Nelson, Flight Stability and Automatic Control, Notre Dame: R. R. Donnelley & Sons Company, 1989.

[11] D. J. Roskam, "Flying Qualities MIL-F-8785C," in Airplane Design Part-1, 1995.

[12] Nguyen tien Dat, Tran Ngoc Son and Duong Anh Tra, "Development of a Flight Dynamics model for fixed wing aircraft," in ICCMS, Sydney, Australia, 2018.

[13] Geoffrey Larkin and Graham Coates, "A Design Analysis of Vertical Stabilizers for Blended Wing Body Aircraft" in School of Engineering and Computing Sciences, Durham University, Durham, UK, 2 February 2017.

[14] D. R. C. Nelson, Flight Stability and Automatic Control, R R donnelley and Sons Company.

[15] Vinayagam A. K. and Nandan K. Sinha, "An Assessment of Thrust Vector Concepts for Twin Engine Airplane," Journal of Aerospace Engineering, April 2013.

[16] M. Sadraey and R. Colgren, "A Systems Engineering Methodology for the Design of Unconventional Control Surfaces," in AIAA, 10 January 2008.

[17] A. Bhatt, M. Harvey and R. Hofmeister "Geometric and Computer Analysis of F-35A lightning II," 2012.

[18] P. E. Purser and J. P. Campbell, "Experimental Verification of a Simplified Vee-Tail Theory and Analysis of Available Data on Complete Models with Vee Tails," NACA TR-823.

[19] W. F. Phillips and D. O. Synder, "Modern Adaptation of Prandtl's ClassicLifting-LineTheory," Journal of Aircraft," AIAA, pp. 662-670, 2000.

[20] L. Garcia-Harnandez, C. Cuerno-Rejado and M. Perez-Cortes "Dynamics and Failure Models for a V-Tail Remotely Piloted Aircraft System," Journal of Guidance, Control and Dynamics, 2015.

[21] The Mathworks Inc., MATLAB/Simulink, Software Package, Version 2017b.

[22] http://www.gulfstream.com/aircraft/gulfstream-g550

[23] D. P. Raymer, Aircraft Design: A Conceptual Approach, Sylmar, California: Air Force Institute of Technology, 1989.

[24] W. E. a. H. C. E. Philips, "Review of Attitude Representations Used for Aircraft Kinematics," *AIAA Journal of Aircraft*, vol. 38, no. 4, 2008.

[25] B. P. Icker, "A New Method for Performing Digital Control System Attitude Computations Using Quaternions," in *AIAA Guidance, Control, and Flight Dynamics Conference*, Pasadena, CA, 1968.

[26] J. M. Z. M. J. P. D. R. a. M. R. B. Cooke, "NPSNET Flight Simulation Dynamic Modeling Using Quaternions," *Presence*, vol. 1, no. 4, pp. 404-420, 1994.

[27] H. I. Leong, "Development of a 6DOF Nonlinear Simulation Model Enhanced with Fine Tuning Procedures," University of Kansas, 2008.

[28] U. O. E. M. J. M. Kavsaoglu, "Calculation of the Longitudinal Stability Derivatives of a Transport Aircraft and Analysis of Longitudinal Modes," in Proceedings of the 9th WSEAS International Conference on Automatic Control, Modeling and Simulation, Isantbul, Turkey, 2007.

[29] H. e. al., "Dynamic Stability," in Stability Characteristics of Boeing 747, pp. 101-102.

[30] M. F. R. Nurbaiti Wahid, "Pitch Control System Using LQR and Fuzzy Logic Controller," in IEEE Symposium on Industrial Electronics and Application (ISIEA 2010), Penang, 2010.

CERTIFICATE OF COMPLETENESS

It is hereby certified that the dissertation submitted by NS Muhammad Uzair Khan, Reg No. **00000171149**, Titled: ***Simulation and Mathematical Modelling of Aircraft Flying Qualities with Varying Tail Dihedral*** has been checked/reviewed and its contents are complete in all respects.

Supervisor's Name: **Dr. Naveed A. Din** Signature: _____

Date: _____